Figure 5. Lymph node macrophages are highly responsive to TLR agonists. (a) Incorporation of subcutaneously injected, FITC-labeled CpG ODN into macrophages and DCs in the DLN. BALB/c mice (two mice per group) were injected with FITC-CpG ODN (50 μg), and 16 h later, macrophages (F4/80$^+$CD11b$^+$) and DCs (CD11c$^+$F4/80$^-$) in the DLN were isolated, and uptake of FITC-CpG ODN in these cells was measured using flow cytometry. (b) Activation of macrophages and DCs in the DLN by TLR agonists. BALB/c mice (two mice per group) were subcutaneously injected with CpG ODN (50 μg) or poly-ICLC RNA (50 μg), and 16 h later, macrophages and DCs in the DLN were tested for expression of CD80 and CD86. MFI, mean fluorescence intensity.

molecules CD80 and CD86. In accordance with the uptake of CpG ODN, the up-regulation of CD80 and CD86 by TLR stimulation was prominent in macrophages (Figure 5b). These data revealed that lymph node macrophages are highly responsive to TLR stimulation, and possibly this way they acquire the high cross-presenting activity. Therefore, concurrent, appropriate TLR stimulation would be a prerequisite for the activity of macrophage-dependent CHP nanogel-based vaccine. Conversely, thanks to the high susceptibility of lymph node macrophages to TLR stimulation, the CHP nanogel-based vaccine would acquire its high potency.

DISCUSSION

Thus far, no antigen delivery system targeting macrophages localized in the lymph node has been available, although several vaccine formulations selective for splenic macrophages have been developed including a micropaticulate antigen with a diameter of 0.5 μm for MARCO$^+$ macrophages[31] and an anti-CD169 antibody-fused protein antigen for CD169$^+$ macrophages.[32] The present study showed for the first time that the CHP nanogel functions as a lymph node medullary macrophage-selective vaccine delivery system. A precise mechanism for the preferential incorporation of the CHP nanogel into medullary macrophages has yet to be elucidated, but the unique characteristics of CHP nanogel may help to explain that phenomenon. Because the CHP nanogel is immunologically inert, immune cells including DCs would not be able to sense and engulf the nanogel. Nevertheless, medullary macrophages can, likely due to their very high phagocytic activity.[22] Thus, the CHP nanogel-based vaccine likely acquires its macrophage-selective delivery function as a consequence of avoiding surveillance by other cells (the "immunologically

stealth vaccine"). The difference between medullary and subcapsular sinus macrophages also may be explained by a similar reason.[22] The present study also validated a novel approach to give a material a delivery function targeting a certain immune cell population by strictly preventing acquisition by unintended cells.

The functions of medullary macrophages that involve scavenging of pathogens and particulate antigens from the lymph and supporting plasma-cell survival have been reported,[22] but their involvement in the induction of T cell response has been unexplored. To our knowledge, the present study is the first report describing the participation of medullary macrophages in T cell immunity. Cross-presentation by these macrophages required the presence of TLR agonist probably because the TLR stimulation upregulated the phagocytic, antigen processing, and/or presenting functions of these macrophages. On the other hand, it is also possible that TLR stimulation attenuates cross-presentation, because TLR stimulation is also known to increase the digestive activity of phagosomes that destroys antigens,[33] which can result in destruction of putative epitopes. Medullary macrophages may possess some intrinsic mechanism to avoid this effect, for example, increased escape of antigens from phagosomes to the cytosol.[34] Alternatively, the CHP nanogel may protect antigens from excess degradation in phagosomes. We also confirmed that similar to murine macrophages, human macrophages were also highly capable of cross-presenting antigens but only in the presence of TLR stimulation (Supporting Information, Figure S9). To further evaluate the significance of cross-presentation by lymph node macrophages and to harness it for effective tumor vaccination, the direct and/or indirect mechanisms by which TLR stimulation regulates the quality

- 19 -

and outcome of macrophage-mediated cross-presentation should be clarified in the future.

CONCLUSION

The present study demonstrated that selective vaccine delivery to medullary macrophages localized in the medulla, the core of lymph nodes, can be achieved by using an immunologically stealth nanoparticulate delivery system. We also revealed that medullary macrophages have a potential to effectively induce specific CD8$^+$ T cell response to vaccines. These two key findings build a theoretical basis to design a macrophage-oriented cancer vaccine with high potency, which may overcome the limited clinical efficacy of existing cancer vaccines. This strategy may improve the therapeutic efficacy of vaccines against not only cancers but also infectious diseases reactive to T cell immunity, and may thus have great impact in the field of immunotherapy. Cancer vaccines utilizing the CHP nanogel used in the present study have already been tested in clinical trials and confirmed to be highly safe and immunogenic, also supporting the clinical application of macrophage-oriented vaccines utilizing this nanoparticulate delivery system.

MATERIALS AND METHODS

Fabrication and Analysis of the Complex of CHP Nanogel with LPA. CHP, rhodamine-labeled CHP, CHP-NH$_2$, and CHG were synthesized as described previously.[35−37] LPAs were chemically synthesized by Bio-Synthesis, Inc. (Lewisville, TX). The sequences of the LPAs used were as follows: human MAGE-A4-derived LPA (GSNPARYEFLWGPRALAETSYVKVLEHVVRVNARVRIAYP), mERK2-derived LPA (NDHIAYFLYQILRGLQYIHSANVLHRDLKPSNLLLNT), and human NMW LPA (**SLLMWITQC**YYYYYY**NYKRCFPVI**YYY-YYY**CMTWNQMNL**). The MAGE-A4 LPA and mERK2 LPA contain epitopes for murine CD8$^+$ T cells (underlined), and the human NMW LPA does for HLA-A2-restricted NY-ESO-1, HLA-A24-restricted MAGE-A4, and HLA-A24-restricted WT1 epitopes (bold). For analysis of antigen incorporation, these LPAs were labeled with fluorescein amidite (FAM). LPA and CHP were dissolved in dimethyl sulfoxide and phosphate-buffered saline (PBS) containing 6 M urea, respectively. Both solutions were combined and gently mixed at room temperature, followed by dialysis against PBS to remove urea. The resulting solution of the CHP:LPA complex was stored at 4 °C until use. The peptide concentration in the CHP:LPA complex solution was determined by measuring the absorbance at 280 nm, where CHP does not contribute to absorbance. The final concentration of CHP was approximately 10 mg/mL and that of LPA was 0.2−0.4 mg/mL. Complexation of the CHP nanogel and FAM-labeled LPA was confirmed by means of high performance size exclusion chromatography (HPSEC) using a Superose 12 10/300 GL column (GE Healthcare). An aliquot of the sample was injected into the HPSEC system (Shimadzu), eluted with PBS, and detected by means of ultraviolet absorbance at 495 nm. To determine the size of the CHP nanogel and CHP:LPA complex, dynamic light scattering measurement was performed using a Zetasizer Nano ZS (Malvern Instruments, Ltd.) at 633 nm and a 173° detection angle at 25 °C. The measured autocorrelation function was analyzed using the cumulant method. The hydrodynamic diameter (D_H) of the samples was calculated from the Stokes−Einstein equation. The ζ-potential of CHP:LPA complex was also measured using the Zetasizer Nano ZS at a 90° detection angle at 25 °C in PBS. The mERK2 CHP:LPA complex was also analyzed using transmission electron microscopy (TEM). Briefly, the sample was applied to a carbon-coated grid, and the grid was stained with TI blue (Nisshin EM, Japan), dried, and subjected to TEM (HT7700, Hitachi) at an accelerating voltage of 100 kV.

Mice and Tumors. Female BALB/c mice were obtained from SLC Japan and used at 6−12 weeks of age. DUC18 mice, transgenic for TCRα/β that interacts with a K^d-restricted mERK2$_{136−144}$ peptide epitope, were established as described previously.[25] CD90.1-congenic BALB/c mice were kindly provided by Dr. Sakaguchi of Osaka University, Japan. We mated DUC18 mice and CD90.1-congenic mice at our animal facility, and obtained DUC18/CD90.1 mice. T cells isolated from these mice can be traced in *in vitro* and *in vivo* experiments using anti-CD90.1 antibody. All mice were maintained at the Experimental Animal Facility of Mie University. The experimental protocol was approved by the Ethics Review Committee for Animal Experimentation of Mie University.

CT26 is a colon epithelial tumor cell line that was produced by intrarectally injecting N-nitroso-N-methylurethane in BALB/c mice.[30] CT26 cells stably expressing human cancer/testis antigen MAGE-A4 (CT26/MAGE-A4) were established as described previously.[21] CMS5a is a subclone derived from CMS5, a 3-methylcholanthrene-induced sarcoma cell line of BALB/c origin, and expresses mERK2 as a neoantigen.[20] In *in vivo* tumor growth experiments, mice ($n = 4$ or more) were inoculated subcutaneously in the right hind flank with 10^6 CT26/MAGE-A4 or CMS5a cells and monitored three times a week. The tumor size was estimated using the following formula: tumor size (mm^3) = 1/2[length (mm) × width (mm) ^{2}].

Tracking of the Subcutaneously Injected CHP or CHP:LPA Complex. For tracking of the injected CHP nanogel, rhodamine-labeled CHP nanogel was subcutaneously injected to the back of BALB/c mice. Six hours later, the skin harboring DLN was harvested and observed using confocal laser scanning microscope (LSM780, Carl Zeiss, Germany). For tracking of the injected CHP:LPA, a fluorescently labeled LPA complexed with the CHP nanogel was subcutaneously injected into the right hind flank of the mice. The inguinal DLN was harvested 16 h after the injection, mashed, and filtered through a nylon mesh. The resulting cell suspension was analyzed using flow cytometry for incorporation of labeled LPA and expression of CD11b, CD11c, CD169, F4/80, CD3ε, and B220. For immunohistochemical analysis, cryosections were prepared from the DLN. Optimum cutting temperature (O.C.T.) compound-embedded cryosections were stained with fluorescent dye-conjugated anti-CD169 or anti-F4/80 monoclonal antibodies (mAbs) and examined under a fluorescence microscope (BX53F, Olympus).

Immunization of Mice. The CHP:LPA complex or LPA emulsified with IFA (Sigma-Aldrich) was subcutaneously injected into the back of mice at the dose of 50 μg as LPA. Phosphorothioate-containing CpG ODN 1668 (Hokkaido System Science, Japan) or poly-ICLC RNA (Oncovir, Inc.) was simultaneously and subcutaneously injected near the site of vaccination. To deplete macrophages, a clodronate liposome solution (FormuMax Scientific) was subcutaneously injected into the footpad of mice 6 days prior to immunization.

Flow Cytometric Analysis. Fluorescent dye-conjugated mAbs including anti-CD8 (53−6.7), anti-CD4 (RM4−5), anti-interferon (IFN)-γ (XMG1.2), anti-CD80 (2D10.4), anti-CD86 (IT2.2), anti-CD11b (M1/70), anti-CD11c (N418), anti-F4/80 (BM8), anti-CD3ε (145−2C11), anti-CD45R/B220 (RA3−6B2), and anti-CD169 (3D6.112) were purchased from Biolegend. The cell suspension prepared from the inguinal DLN or spleen was stained for surface markers using antibodies at the appropriate concentrations in PBS containing 2% fetal bovine serum for 15 min at 4 °C, and analyzed on a FACSCanto II system (BD Biosciences). For intracellular cytokine staining, splenocytes were incubated with mERK2 LPA or MAGE-A4 LPA for 1 h at 37 °C and then incubated for an additional 6 h with GolgiPlug (BD Bioscience). After permeabilization and fixation using the

- 20 -

Cytofix/Cytoperm Kit (BD Bioscience), the cells were stained with allophycocyanin-conjugated anti-IFN-γ mAb and analyzed using flow cytometry.

T Cell Proliferation and IFN-γ Release Assay. For *in vitro* T cell proliferation assay, the CHP:mERK2 LPA and CpG ODN were subcutaneously injected into the footpad of mice. DLN was resected 20 h after the injection. To isolate CD11b$^+$ cells, the total cell suspension prepared from the DLN was mixed with anti-CD11b microbeads (Miltenyi Biotec) and separated by positive selection on a magnetic bead column. For further fractionation of CD11b$^+$ cells, the cells were stained with FAM-labeled anti-CD11b, PE-labeled anti-CD169, PerCP-Cy5.5-labeled anti-F4/80, and allophycocyanin-labeled anti-CD11c mAbs, and sorted using a FACSAria system (BD Biosciences). The isolated cells (0.1, 0.3, or 1×10^5) were then cocultured with 2.5×10^5 DUC18 T cells prelabeled with carboxyfluorescein succinimidyl ester (CFSE) for 48 h. The dilution of CFSE was measured using flow cytometry to determine cell proliferation. IFN-γ release into the culture medium at 48 h was quantified using a mouse IFN-γ ELISA kit (BD Bioscience).

For *in vivo* T cell proliferation assay, either the CHP:mERK2 LPA or IFA:mERK2 LPA was subcutaneously injected into the back of mice. At day 0 or day 4, 2.5×10^5 DUC18 T cells prelabeled with CFSE were intravenously infused into the vaccinated mice. DLNs were collected on day 3 or day 7, and dilution of CFSE was measured using flow cytometry to determine the *in vivo* proliferation of DUC18 T cells.

In Vitro Cross-Presentation by Human Macrophages. Peripheral blood mononuclear cells were isolated from buffy coats prepared using density gradient centrifugation of the blood of HLA-A0201-positive healthy donors over Ficoll. CD14$^+$ cells were purified with anti-CD14 microbeads and then incubated with GM-CSF, 20 ng/mL in the X-VIVO15 medium, for 7 days to induce differentiation to macrophages. The obtained macrophages were pulsed with human CHP:NMW LPA (10 μg/mL) and stimulated with poly-ICLC RNA (10 μg/mL). The human IFN-γ enzyme-linked immunospot (ELISPOT) assay was performed as previously described. Briefly, a 96-well nitrocellulose ELISPOT plate (Millipore) was coated with an anti-human IFN-γ mAb (clone 1-D1K, Mabtech) overnight at 4 °C. The wells were washed with PBS containing 0.01% Tween 20 (PBS-T) and blocked with the RPMI1640 medium containing 10% fetal calf serum for 2 h at 37 °C. HLA-A0201-restricted NY-ESO-1 epitope-specific CD8$^+$ T cells (clone 1G4, 10^5 cells per well) and antigen-pulsed macrophages were seeded into each well. After incubation for 22 h at 37 °C in 5% CO$_2$, the plate was washed thoroughly with PBS-T. A biotin-conjugated anti-human IFN-γ mAb (clone 7-B6-1, Mabtech) was then added (final concentration 1.25 μg/mL), and the plate was incubated overnight at 4 °C. After a wash step with PBS-T, a streptavidin-alkaline phosphatase conjugate (1 μg/mL; Roche Diagnostics) was added. After incubation for 60 min at room temperature, the wells were washed thrice with PBS-T and stained using an alkaline phosphatase conjugate substrate kit (Life Technologies). The reaction was stopped by intensive washing with distilled water. After the plate dried out, the number of spots in each well was counted using an ELISPOT reader (Cellular Technologies, Ltd.).

Statistical Analysis. The data were analyzed using Student's t test, Dunnett's multiple comparison test, or Tukey-Kramer multiple comparison test. Differences with $p < 0.05$ were considered statistically significant.

Conflict of Interest: The authors declare the following competing financial interest(s): Naozumi Harada is an employee of ImmunoFrontier, Inc. The other authors have no conflicts of interest.

REFERENCES AND NOTES

1. Reddy, S. T.; van der Vlies, A. J.; Simeoni, E.; Angeli, V.; Randolph, G. J.; O'Neil, C. P.; Lee, L. K.; Swartz, M. A.; Hubbell, J. A. Exploiting Lymphatic Transport and Complement Activation in Nanoparticle Vaccines. *Nat. Biotechnol.* **2007**, *25*, 1159–1164.
2. Kourtis, I. C.; Hirosue, S.; de Titta, A.; Kontos, S.; Stegmann, T.; Hubbell, J. A.; Swartz, M. A. Peripherally Administered Nanoparticles Target Monocytic Myeloid Cells, Secondary Lymphoid Organs and Tumors in Mice. *PLoS One* **2013**, *8*, e61646.
3. Kobiyama, K.; Aoshi, T.; Narita, H.; Kuroda, E.; Hayashi, M.; Tetsutani, K.; Koyama, S.; Mochizuki, S.; Sakurai, K.; Katakai, Y.; *et al.* Nonagonistic Dectin-1 Ligand Transforms CpG into a Multitask Nanoparticulate TLR9 Agonist. *Proc. Natl. Acad. Sci. U.S.A.* **2014**, *111*, 3086–3091.
4. Li, A. V.; Moon, J. J.; Abraham, W.; Suh, H.; Elkhader, J.; Seidman, M. A.; Yen, M.; Im, E. J.; Foley, M. H.; Barouch, D. H.; *et al.* Generation of Effector Memory T Cell-Based Mucosal and Systemic Immunity with Pulmonary Nanoparticle Vaccination. *Sci. Transl. Med.* **2013**, *5*, 204–130.
5. Schlosser, E.; Mueller, M.; Fischer, S.; Basta, S.; Busch, D. H.; Gander, B.; Groettrup, M. TLR Ligands and Antigen Need to Be Coencapsulated into the Same Biodegradable Microsphere for the Generation of Potent Cytotoxic T Lymphocyte Responses. *Vaccine* **2008**, *26*, 1626–1637.
6. Trombetta, E. S.; Mellman, I. Cell Biology of Antigen Processing *in Vitro* and *in Vivo*. *Annu. Rev. Immunol.* **2005**, *23*, 975–1028.
7. Asano, K.; Nabeyama, A.; Miyake, Y.; Qiu, C. H.; Kurita, A.; Tomura, M.; Kanagawa, O.; Fujii, S.; Tanaka, M. CD169-Positive Macrophages Dominate Antitumor Immunity by Crosspresenting Dead Cell-Associated Antigens. *Immunity* **2011**, *34*, 85–95.
8. Schliehe, C.; Redaelli, C.; Engelhardt, S.; Fehlings, M.; Mueller, M.; van Rooijen, N.; Thiry, M.; Hildner, K.; Weller, H.; Groettrup, M. CD8$^-$ Dendritic Cells and Macrophages Cross-Present Poly(D,L-Lactate-*co*-Glycolate) Acid Microsphere-Encapsulated Antigen *in Vivo*. *J. Immunol.* **2011**, *187*, 2112–2121.
9. Sasaki, Y.; Akiyoshi, K. Nanogel Engineering for New Nanobiomaterials: from Chaperoning Engineering to Biomedical Applications. *Chem. Rec.* **2010**, *10*, 366–376.
10. Akiyoshi, K.; Deguchi, S.; Moriguchi, N.; Yamaguchi, S.; Sunamoto, J. Self-Aggregates of Hydrophobized Polysaccharides in Water. *Macromolecules* **1993**, *26*, 3062–3068.
11. Akiyoshi, K.; Deguchi, S.; Tajima, T.; Nishikawa, T.; Sunamoto, J. Microscopic Structure and Thermoresponsiveness of a Hydrogel Nanoparticle by Self-Assembly of a Hydrophobized Polysaccharide. *Macromolecules* **1997**, *30*, 857–861.
12. Sasaki, Y.; Iida, D.; Takahashi, H.; Sawada, S.; Akiyoshi, K. Artificial Chaperone Polysaccharide Nanogels for Protein Delivery: a Thermodynamic Study of Protein-Nanogel Interactions Using Fluorescence Correlation Spectroscopy. *Curr. Drug Discovery Technol.* **2011**, *8*, 308–313.
13. Shimizu, T.; Kishida, T.; Hasegawa, U.; Ueda, Y.; Imanishi, J.; Yamagishi, H.; Akiyoshi, K.; Otsuji, E.; Mazda, O. Nanogel DDS Enables Sustained Release of IL-12 for Tumor Immunotherapy. *Biochem. Biophys. Res. Commun.* **2008**, *367*, 330–335.
14. Alles, N.; Soysa, N. S.; Hussain, M. D.; Tomomatsu, N.; Saito, H.; Baron, R.; Morimoto, N.; Aoki, K.; Akiyoshi, K.; Ohya, K. Polysaccharide Nanogel Delivery of a TNF-α and RANKL Antagonist Peptide Allows Systemic Prevention of Bone Loss. *Eur. J. Pharm. Sci.* **2009**, *37*, 83–88.
15. Ikuta, Y.; Katayama, N.; Wang, L.; Okugawa, T.; Takahashi, Y.; Schmitt, M.; Gu, X.; Watanabe, M.; Akiyoshi, K.; Nakamura, H.; *et al.* Presentation of a Major Histocompatibility Complex Class 1-Binding Peptide by Monocyte-Derived Dendritic Cells Incorporating Hydrophobized Polysaccharide-Truncated HER2 Protein Complex: Implications for a Polyvalent Immuno-Cell Therapy. *Blood* **2002**, *99*, 3717–3724.
16. Hasegawa, K.; Noguchi, Y.; Koizumi, F.; Uenaka, A.; Tanaka, M.; Shimono, M.; Nakamura, H.; Shiku, H.; Gnjatic, S.; Murphy, R.; *et al. In Vitro* Stimulation of CD8 and CD4 T

- 21 -

Cells by Dendritic Cells Loaded with a Complex of Cholesterol-Bearing Hydrophobized Pullulan and NY-ESO-1 Protein: Identification of a New HLA-DR15-Binding CD4 T-Cell Epitope. *Clin. Cancer Res.* **2006**, *12*, 1921–1927.

17. Kageyama, S.; Wada, H.; Muro, K.; Niwa, Y.; Ueda, S.; Miyata, H.; Takiguchi, S.; Sugino, S. H.; Miyahara, Y.; Ikeda, H.; *et al.* Dose-Dependent Effects of NY-ESO-1 Protein Vaccine Complexed with Cholesteryl Pullulan (CHP-NY-ESO-1) on Immune Responses and Survival Benefits of Esophageal Cancer Patients. *J. Transl. Med.* **2013**, *11*, 246–255.

18. Kaneo, Y.; Tanaka, T.; Nakano, T.; Yamaguchi, Y. Evidence for Receptor-Mediated Hepatic Uptake of Pullulan in Rats. *J. Controlled Release* **2001**, *70*, 365–373.

19. Coulstock, E.; Sosabowski, J.; Ovecka, M.; Prince, R.; Goodall, L.; Mudd, C.; Sepp, A.; Davies, M.; Foster, J.; Burnet, J.; *et al.* Liver-Targeting of Interferon-Alpha with Tissue-Specific Domain Antibodies. *PLoS One* **2013**, *8*, e57263.

20. Ikeda, H.; Ohta, N.; Furukawa, K.; Miyazaki, H.; Wang, L.; Kuribayashi, K.; Old, L. J.; Shiku, H. Mutated Mitogen-Activated Protein Kinase: a Tumor Rejection Antigen of Mouse Sarcoma. *Proc. Natl. Acad. Sci. U.S.A.* **1997**, *94*, 6375–6379.

21. Muraoka, D.; Nishikawa, H.; Noguchi, T.; Wang, L.; Harada, N.; Sato, E.; Luescher, I.; Nakayama, E.; Kato, T.; Shiku, H. Establishment of Animal Models to Analyze the Kinetics and Distribution of Human Tumor Antigen-Specific CD8^{+} T Cells. *Vaccine* **2013**, *31*, 2110–2118.

22. Gray, E. E.; Cyster, J. G. Lymph Node Macrophages. *J. Innate Immun.* **2012**, *4*, 424–436.

23. Coffman, R. L.; Sher, A.; Seder, R. A. Vaccine Adjuvants: Putting Innate Immunity to Work. *Immunity* **2010**, *33*, 492–503.

24. Huang, X.; Yang, Y. Targeting the TLR9-MyD88 Pathway in the Regulation of Adaptive Immune Responses. *Expert Opin. Ther. Targets* **2010**, *14*, 787–796.

25. Hanson, H. L.; Donermeyer, D. L.; Ikeda, H.; White, J. M.; Shankaran, V.; Old, L. J.; Shiku, H.; Schreiber, R. D.; Allen, P. M. Eradication of Established Tumors by CD8^{+} T Cell Adoptive Immunotherapy. *Immunity* **2000**, *13*, 265–276.

26. Barral, P.; Polzella, P.; Bruckbauer, A.; van Rooijen, N.; Besra, G. S.; Cerundolo, V.; Batista, F. D. CD169^{+} Macrophages Present Lipid Antigens to Mediate Early Activation of iNKT Cells in Lymph Nodes. *Nat. Immunol.* **2010**, *11*, 303–312.

27. Hailemichael, Y.; Dai, Z.; Jaffarzad, N.; Ye, Y.; Medina, M. A.; Huang, X. F.; Dorta-Estremera, S. M.; Greeley, N. R.; Nitti, G.; Peng, W.; *et al.* Persistent Antigen at Vaccination Sites Induces Tumor-Specific CD8^{+} T Cell Sequestration, Dysfunction and Deletion. *Nat. Med.* **2013**, *19*, 465–472.

28. DeLeo, A. B.; Shiku, H.; Takahashi, T.; John, M.; Old, L. J. Cell Surface Antigens of Chemically Induced Sarcomas of the Mouse. I. Murine Leukemia Virus-Related Antigens and Alloantigens on Cultured Fibroblasts and Sarcoma Cells: Description of a Unique Antigen on BALB/c Meth A Sarcoma. *J. Exp. Med.* **1997**, *146*, 720–734.

29. Muraoka, D.; Kato, T.; Wang, L.; Maeda, Y.; Noguchi, T.; Harada, N.; Takeda, K.; Yagita, H.; Guillaume, P.; Luescher, I.; *et al.* Peptide Vaccine Induces Enhanced Tumor Growth Associated with Apoptosis Induction in CD8^{+} T Cells. *J. Immunol.* **2010**, *185*, 3768–3776.

30. Griswold, D. P.; Corbett, T. H. A Colon Tumor Model for Anticancer Agent Evaluation. *Cancer* **1975**, *36*, 2441–2444.

31. Getts, D. R.; Martin, A. J.; McCarthy, D. P.; Terry, R. L.; Hunter, Z. N.; Yap, W. T.; Getts, M. T.; Pleiss, M.; Luo, X.; King, N. J.; *et al.* Microparticles Bearing Encephalitogenic Peptides Induce T-Cell Tolerance and Ameliorate Experimental Autoimmune Encephalomyelitis. *Nat. Biotechnol.* **2012**, *30*, 1217–1224.

32. Backer, R.; Schwandt, T.; Greuter, M.; Oosting, M.; Jüngerkes, F.; Tüting, T.; Boon, L.; O'Toole, T.; Kraal, G.; Limmer, A.; *et al.* Effective Collaboration Between Marginal Metallophilic Macrophages and CD8^{+} Dendritic Cells in the Generation of Cytotoxic T Cells. *Proc. Natl. Acad. Sci. U.S.A.* **2010**, *107*, 216–221.

33. Blander, J. M. Phagocytosis and Antigen Presentation: a Partnership Initiated by Toll-Like Receptors. *Ann. Rheum. Dis.* **2008**, *67*, iii44–49.

34. Segura, E.; Durand, M.; Amigorena, S. Similar Antigen Cross-Presentation Capacity and Phagocytic Functions in All Freshly Isolated Human Lymphoid Organ-Resident Dendritic Cells. *J. Exp. Med.* **2013**, *210*, 1035–1047.

35. Akiyoshi, K.; Kobayashi, S.; Shichibe, S.; Mix, D.; Baudys, M.; Kim, S. W.; Sunamoto, J. Self-Assembled Hydrogel Nanoparticle of Cholesterol-Bearing Pullulan as a Carrier of Protein Drugs: Complexation and Stabilization of Insulin. *J. Controlled Release* **1998**, *54*, 313–320.

36. Ayame, H.; Morimoto, N.; Akiyoshi, K. Self-Assembled Cationic Nanogels for Intracellular Protein Delivery System. *Bioconjugate Chem.* **2008**, *19*, 882–890.

37. Takeda, S.; Takahashi, H.; Sawada, S.; Sasaki, S.; Akiyoshi, K. Amphiphilic Nanogel of Enzymatically Synthesized Glycogen as an Artificial Molecular Chaperone for Effective Protein Refolding. *RSC Adv.* **2013**, *3*, 25716–25718.

- 22 -

Nonagonistic Dectin-1 ligand transforms CpG into a multitask nanoparticulate TLR9 agonist

Kouji Kobiyama[a,b], Taiki Aoshi[a,b], Hirotaka Narita[c], Etsushi Kuroda[a,b], Masayuki Hayashi[a,b], Kohhei Tetsutani[a,b], Shohei Koyama[d,e], Shinichi Mochizuki[f], Kazuo Sakurai[f], Yuko Katakai[g], Yasuhiro Yasutomi[h], Shinobu Saijo[i,j], Yoichiro Iwakura[k], Shizuo Akira[l], Cevayir Coban[m], and Ken J. Ishii[a,b,1]

[a]Laboratory of Adjuvant Innovation, National Institute of Biomedical Innovation, Osaka 567-0085, Japan; Laboratories of [b]Vaccine Science, [l]Host Defense, and [m]Malaria Immunology, World Premier International Immunology Frontier Research Center and [c]Supramolecular Crystallography, Research Center for Structural and Functional Proteomics, Institute for Protein Research, Osaka University, Osaka 565-0871, Japan; [d]Department of Medical Oncology and [e]Cancer Vaccine Center, Dana-Farber Cancer Institute, Boston, MA 02115; [f]Department of Chemistry and Biochemistry, University of Kitakyushu, Fukuoka 808-0135, Japan; [g]Corporation for Production and Research of Laboratory Primates, Ibaraki 305-0843, Japan; [h]Tsukuba Primate Research Center, National Institute of Biomedical Innovation, Ibaraki 305-0843, Japan; [i]Department of Molecular Immunology, Medical Mycology Research Center, Chiba University, Chiba 260-8673, Japan; [j]Precursory Research for Embryonic Science and Technology, Japan Science and Technology Agency, Saitama 332-0012, Japan; and [k]Division of Experimental Animal Immunology, Research Institute for Biomedical Sciences, Tokyo University of Science, Chiba 278-8510, Japan

CpG DNA, a ligand for Toll-like receptor 9 (TLR9), has been one of the most promising immunotherapeutic agents. Although there are several types of potent humanized CpG oligodeoxynucleotide (ODN), developing "all-in-one" CpG ODNs activating both B cells and plasmacytoid dendritic cells forming a stable nanoparticle without aggregation has not been successful. In this study, we generated a novel nanoparticulate K CpG ODN (K3) wrapped by the nonagonistic Dectin-1 ligand schizophyllan (SPG), K3-SPG. In sharp contrast to K3 alone, K3-SPG stimulates human peripheral blood mononuclear cells to produce a large amount of both type I and type II IFN, targeting the same endosome where IFN-α-inducing D CpG ODN resides without losing its K-type activity. K3-SPG thus became a potent adjuvant for induction of both humoral and cellular immune responses, particularly CTL induction, to coadministered protein antigens without conjugation. Such potent adjuvant activity of K3-SPG is attributed to its nature of being a nanoparticle rather than targeting Dectin-1 by SPG, accumulating and activating antigen-bearing macrophages and dendritic cells in the draining lymph node. K3-SPG acting as an influenza vaccine adjuvant was demonstrated in vivo in both murine and nonhuman primate models. Taken together, K3-SPG may be useful for immunotherapeutic applications that require type I and type II IFN as well as CTL induction.

innate immunity | two-photon microscopy | MARCO | Siglec-1 | β-glucan

CpG oligodeoxynucleotide (CpG ODN) is a short (~20 bases), single-stranded synthetic DNA fragment containing the immunostimulatory CpG motif, a potent agonist for Toll-like receptor 9 (TLR9), which activates dendritic cells (DCs) and B cells to produce type I interferons (IFNs) and inflammatory cytokines (1, 2) and acts as an adjuvant toward both Th1-type humoral and cellular immune responses, including cytotoxic T-lymphocyte (CTL) responses (3, 4). Therefore, CpG ODN has been postulated as a possible immunotherapeutic agent against infectious diseases, cancer, asthma, and pollinosis (2, 5).

There are at least four types of CpG ODN, each of which has a different backbone, sequence, and immunostimulatory properties (6). D-type (also called A) CpG ODNs typically comprise one palindromic CpG motif with a phosphodiester (PO) backbone and phosphorothioate (PS) poly(G) tail, and activates plasmacytoid DCs (pDCs) to produce a large amount of IFN-α but fails to induce pDC maturation and B-cell activation (7, 8). The three other types of ODN consist of a PS backbone. K-type (also called B) CpG ODN contains nonpalindromic multiple CpG motifs, and strongly activates B cells to produce IL-6 and pDCs to maturation but barely produces IFN-α (8, 9). Recently, C and P CpG ODNs have been developed; these contain one and two palindromic CpG sequences, respectively, both of which can activate B cells like K-type and pDC like D-type, although C

CpG ODN induces weaker IFN-α production compared with P CpG ODN (10–12).

D and P CpG ODNs have been shown to form higher-order structures, Hoogsteen base pairing to form parallel quadruplex structures called G tetrads, and Watson–Crick base pairing between *cis*- and *trans*-palindromic portions, respectively, that are required for robust IFN-α production by pDCs (12–14). Although such higher-order structures appear necessary for localization to early endosomes and signaling via TLR9, they suffer from product polymorphisms, aggregation, and precipitation, thereby hampering their clinical application (15). Therefore, only K and C CpG ODNs are generally available as immunotherapeutic agents and vaccine adjuvants for human use (16, 17). Although K CpG ODN enhances the immunogenicity of vaccines targeting infectious diseases and cancers in human clinical trials (6, 17), chemical or physical conjugation between antigen and K CpG ODN is necessary for optimal adjuvant effects. These results indicate that these four (K, D, P, and C) types of CpG ODN have advantages and disadvantages; however, the

Significance

CpG oligodeoxynucleotide (ODN), a Toll-like receptor 9 ligand, is a promising immunotherapeutic agent; however, developing an IFN-inducing CpG ODN forming a stable nanoparticle without aggregation has been unsuccessful. Here we generated a nanoparticulate CpG ODN (K3) wrapped by the nonagonistic Dectin-1 ligand schizophyllan (SPG), K3-SPG. K3-SPG stimulates human peripheral blood mononuclear cells to produce large amounts of both type I and II IFN. K3-SPG thus became a potent adjuvant, especially for cytotoxic T-lymphocyte (CTL) induction to coadministered protein antigens without conjugation, which is attributable to its nanoparticulate nature rather than to targeting Dectin-1. Protective potency of K3-SPG as an influenza vaccine adjuvant was demonstrated in both murine and nonhuman primate models. K3-SPG may be used as an IFN inducer as well as a CTL inducer for immunotherapeutic applications.

development of an "all-in-one" CpG ODN activating both B cells and pDCs that forms a stable nanoparticle without aggregation has yet to be accomplished. A better strategy, targeting CpG ODN toward antigen-presenting cells (APCs), is desired to improve immunostimulatory specificity and immunotherapeutic efficacy of CpG ODNs.

Schizophyllan (SPG), a soluble β-glucan derived from *Schizophyllum commune*, is a drug that has been approved in Japan as an enhancer of radiotherapy in cervical carcinoma patients for the last three decades (18). It has been shown to form a complex with polydeoxyadenylic acid (dA) as a triple-helical structure (19). Although we previously demonstrated that mouse and humanized CpG ODN with PO poly(dA) at the 5′ end complexed with SPG enhanced cytokine production and acted as an influenza vaccine adjuvant (20, 21), it has been difficult to achieve high yields of the CpG–SPG complex toward its more efficient and cost-effective preclinical as well as clinical development. Recently, when the PS backbone of the dA sequence was linked to CpG ODN, the efficacy of complex formation was elevated by nearly 100% (22). However, a thorough investigation has yet to be conducted to identify the best humanized CpG sequence and optimization of factors to gain all-in-one activities of the four types of CpG ODN.

To do this, we sought to optimize a humanized CpG–SPG complex as a vaccine adjuvant and immunostimulatory agent in humans (in vitro), mice (in vitro and in vivo), and nonhuman primates (in vivo). In this study, we identified a novel K CpG ODN (K3) and SPG complex, namely K3-SPG. It forms a higher-order nanoparticle that can be completely solubilized. We found that this all-in-one K3-SPG displayed a more potent activity than, and different characteristics from, any other type of CpG ODN and previous CpG–SPG complexes.

Results

A Rod-Shaped Nano-Sized Particle of K3-SPG Gains Dual Characteristics of K- and D-Type CpG ODNs.

To make a complex between CpG ODNs and schizophyllan (SPG), CpG ODNs need additional sequences of phosphorothioate backbone of 40-mer polydeoxyadenylic acid (dA_{40}) at the 5′ or 3′ end (20, 22). Fig. 1*A* shows methods of CpG ODN and SPG complexation through denaturing–renaturing procedures. In this study, we selected K3 as a K-type CpG ODN. At first, we examined the immunostimulatory impacts of the 5′ and 3′ ends of CpG ODN. 5′-K3-dA_{40}-3′, but not 5′-dA_{40}-K3-3′, complexed with SPG-activated human peripheral blood mononuclear cells (PBMCs) to produce a robust amount of IFN-α (Fig. 1*B* and Fig. S1). K3, K3-dA_{40}, or dA_{40}-K3, which are able to activate human PBMCs to produce other cytokines such as IL-6, failed to produce IFN-α (Fig. 1*B* and Fig. S1). These results indicate that the 5′-CpG sequence (K3-SPG) is more desirable than the 3′-CpG sequence as a novel TLR9 agonist. Although some CpG ODN–induced cytokine production is known to have a dose-dependent correlation, K3-SPG–induced IFN-α production is not. Given that previous reports showed that IFN-α production by K CpG ODN stimulation has a bell-shaped dose–response correlation (7), altogether these results suggest that K3-SPG still has the character of K CpG ODN.

Qualification and quantitation of K3-SPG were conducted by scanning electron microscopy (SEM) and dynamic light scattering (DLS). K3-SPG had a rod-like structure, consistent with that seen in a previous report (23) (Fig. 1*C*). It appeared to be a soluble monomeric nanoparticle with an average diameter of 30 nm, comparable to SPG itself and smaller than D CpG ODN (D35) (14, 24) (Fig. 1*D*). Given that K3-SPG forms a nanoparticle, we compared the immunostimulatory activities of K3-SPG with D, C, and P CpG ODNs. PBMCs stimulated with K3-SPG produced larger amounts of IFN-α and IFN-γ but at far lower concentrations than those induced by D35 (Fig. 1*E*) and P and C CpG ODNs (Fig. S2). These results suggest that K3-SPG gains the characteristic of D CpG ODN without losing that of the K type, because these IFNs are known to be D type-specific cytokines (7, 8, 25). To understand the dual functions of K and D
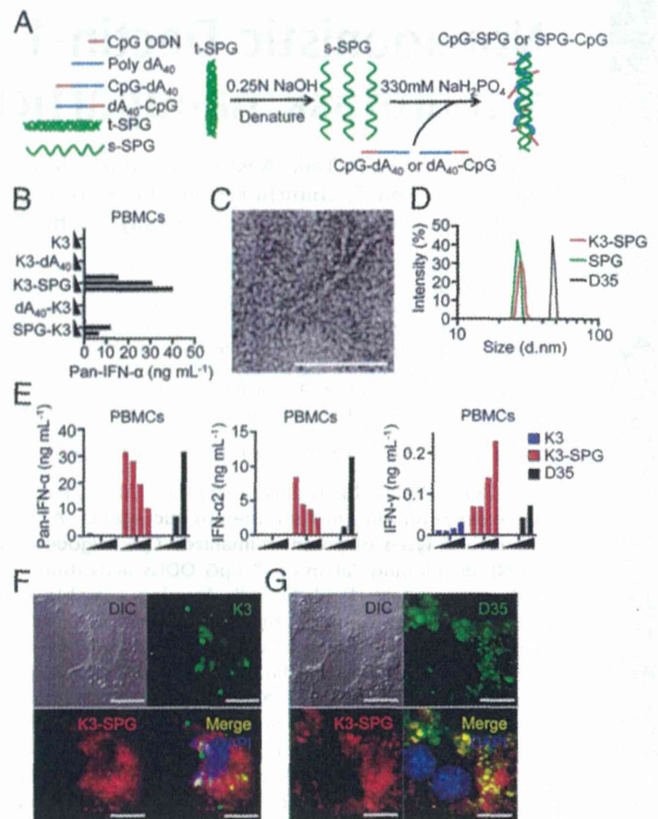

Fig. 1. K (*B*) CpG ODN and SPG complex forms nanoparticles and gains D (*A*) CpG ODN characteristics. (*A*) Methods of CpG ODN and SPG complexation. tSPG, triple-stranded SPG; sSPG, single-stranded SPG. (*B*) Production of IFN-α by human PBMCs stimulated with K3, K3-dA_{40}, K3-SPG, dA_{40}-K3, or SPG-K3 (adjusted for K3 ODN concentration at 0.1, 0.3, or 1 μM) for 24 h was measured by ELISA. (*C*) K3-SPG processed for SEM. (Scale bar, 50 μm.) (*D*) Size of K3-SPG, SPG, and D35 was analyzed by DLS. (*E*) Production of type I and II IFNs by PBMCs stimulated with K3, K3-SPG, or D35 for 24 h was measured by ELISA. (*F* and *G*) Mouse BMDMs were stimulated with Alexa 488-K3 (*F*) or Alexa 488-D35 (*G*) and Alexa 647-K3-SPG at 1 μM for 3 h. The cells were incubated with Hoechst 33258, fixed, and analyzed by fluorescence microscopy. DIC, differential interference contrast. (Scale bars, 10 μm.) Data represent one of three independent experiments with similar results.

CpG ODNs, we analyzed the intracellular localization of K3-SPG in bone marrow-derived macrophages (BMDMs). K3-SPG was colocalized with not only the endosomes containing K CpG ODN but also those containing D CpG ODN (Fig. 1 *F* and *G*) such as C CpG ODN (26), suggesting that K3-SPG may transduce endosome-mediated innate immune signaling pathways by K and D CpG ODNs. These results strongly suggest that K3-SPG forms a nano-sized higher-order and completely solubilized particle and found that this all-in-one K3-SPG displayed a more potent activity than, and different characteristic from, any other CpG ODNs and previously known CpG–SPG complex.

K3-SPG Is a Prominent Vaccine Adjuvant That Induces Potent CTL Responses to Protein Antigen Without Conjugation.

We compared the adjuvant effects of K3, K3-dA_{40}, and K3-SPG in a murine immunization model. When wild-type mice were immunized with LPS-free chicken ovalbumin protein (OVA) alone or OVA with each K3-derived adjuvant, K3-SPG induced significantly higher humoral immune responses (Fig. 2*A*) and stronger T-cell responses than that induced by K3 (Fig. 2*B*). Of note, tetramer assays revealed a significantly greater number of OVA-specific CD8 T cells (Fig. 2*C*). We also observed very strong in vivo CTL activity against
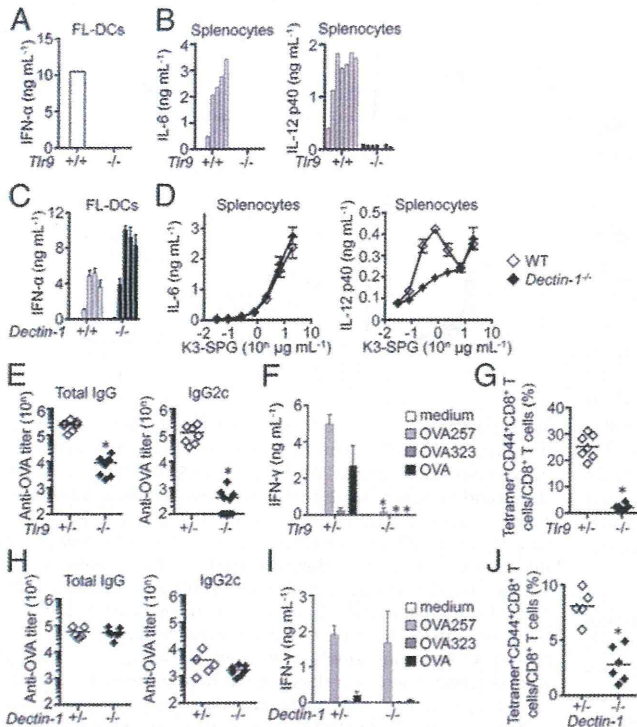
Fig. 4

Fig. 4. Adjuvant effects of K3-SPG were completely dependent on TLR9 and partially on Dectin-1. FL-DCs (*A* and *C*) or splenocytes (*B* and *D*) from C57BL/6J, *Tlr9*$^{-/-}$, or *Dectin-1*$^{-/-}$ mice were stimulated with K3-SPG [20 μg/mL (*A*), 0.014–10 μg/mL (*B*), or 0.014–10 μg/mL (*C* and *D*)] for 24 h, and their cytokine production was monitored by ELISA. *Tlr9*$^{+/-}$ (*n* = 7) or *Tlr9*$^{-/-}$ mice (*n* = 10) (*E*–*G*) and *Dectin-1*$^{+/-}$ (*n* = 5) or *Dectin-1*$^{-/-}$ mice (*n* = 6) (*H*–*J*) were immunized s.c. with OVA (100 μg) and K3-SPG [10 μg (*E*–*G*) or 1 μg (*H*–*J*)] at days 0 and 10. Seven days after the last immunization, OVA-specific serum IgG (*E* and *H*), IFN-γ (*F* and *I*), and OVA$_{257-264}$-specific tetramer (*G* and *J*) were monitored. *P < 0.05 (Mann–Whitney *U* test). Data represent one of two or three independent experiments with similar results.

base of the tail, both antigen and adjuvant reached the surface of draining inguinal lymph nodes (iLNs) within 1 h (Fig. 5 *A*, *B*, and *D*). After 24 h, some K3-SPG had moved to the CD3e$^+$ T-cell area and colocalized with DQ-OVA (Fig. S6*A*). Those cells that contained both K3-SPG and DQ-OVA in the T-cell area of the iLNs were CD11c$^+$ DCs (Fig. S6*B*).

Of interest, the majority of fluorescence signals remained on the surface of the iLNs (Fig. 5*A*), prompting us to focus on two types of macrophages known to be distributed on the LN surface, Siglec-1$^+$ (also called CD169 or MOMA-1) macrophages (also known as subcapsular sinus macrophages) and MARCO$^+$ macrophages (31). Histological analysis using conventional fluorescence microscopy did not suitably reveal the entire iLN surface; moreover, these macrophages were difficult to isolate for flow cytometric analysis (32, 33). Hence, we used two-photon microscopy imaging analysis to clarify the distribution of antigen and K3-SPG ex vivo. After the injection of anti-MARCO and –Siglec-1 antibodies, specific macrophages were visualized (Movie S1). When the iLN surface was monitored by two-photon microscopy at 1 h postinjection, OVA and K3-SPG were colocalized with MARCO$^+$ but not Siglec-1$^+$ macrophages (Fig. 5 *B* and *D*, Fig. S7 *A*–*D*, and Movies 2–5). Previous reports suggest that the immune complex and inactivated influenza virus are captured by Siglec-1$^+$ macrophages to induce humoral immune responses (34, 35). The distribution pattern perfectly matched that for MARCO$^+$ macrophages in the iLNs and did not colocalize with Siglec-1$^+$ macrophages, as confirmed by Volocity's colocalization analysis (Perkin Elmer) (Fig. 5 *B*–*E*). In contrast, K3 was more

diffusely distributed between MARCO$^+$ and Siglec-1$^+$ areas compared with K3-SPG (Fig. 5 *D* and *E*, Fig. S7 *C*–*E*, and Movies 6 and 7). Additionally, both *Tlr9*- and *Dectin-1*–deficient mice showed comparable localization of K3-SPG (Fig. S7 *F* and *G*).

To determine the contribution of these macrophages toward the adjuvant effects of K3-SPG, we examined different recovery kinetics of macrophages and DCs following an injection of clodronate liposomes into the base of the tail. After the injection, the macrophages were completely depleted by day 2. These cells did not recover for at least 1 wk, whereas DCs were mostly recovered by day 7, as previously reported (36). When both macrophages and DCs were depleted, immune responses were significantly suppressed [Fig. 5*F*, Clo (−d2)]. When only macrophages, but not DCs, were depleted, the immune responses were comparable to those in untreated mice [Fig. 5*F*, Clo (−d7)]. This would suggest that although both OVA and K3-SPG were mainly captured by
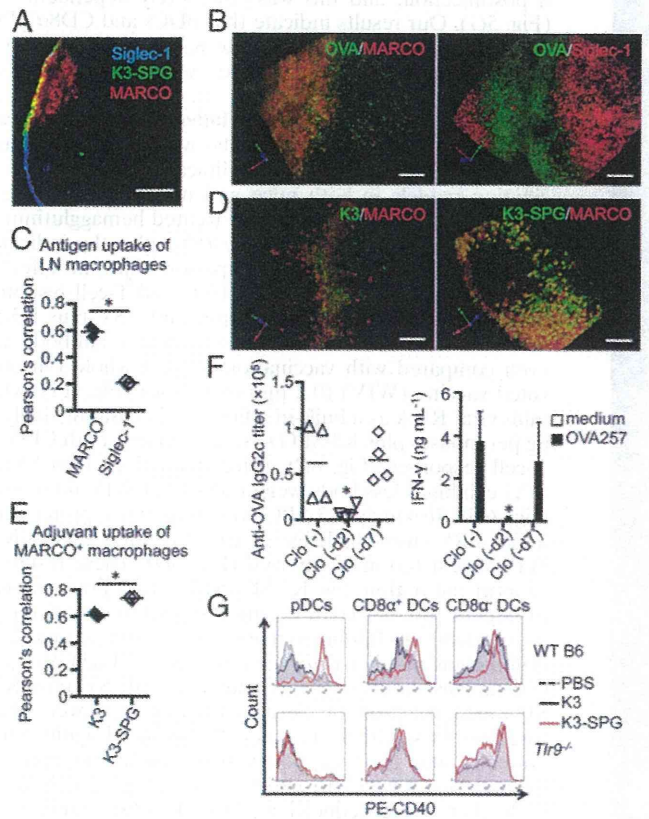
Fig. 5

Fig. 5. Role of lymph node macrophages and dendritic cells in uptake and adjuvant effects of K3-SPG. (*A*) Immunohistochemistry of mouse inguinal LNs after Alexa 488-K3-SPG injection. One hour after injection, the LNs were collected and stained with anti–MARCO-phycoerythrin (PE) and anti–Siglec-1-APC antibodies. (*B*–*E*) Two-photon microscopic analysis of LNs. DQ-OVA, Alexa 488-K3, or Alexa 488-K3-SPG was injected as indicated, and anti–MARCO-PE or anti–Siglec-1-PE antibodies were administered. The LNs were collected 1 h later and analyzed by two-photon microscopy. (*C* and *E*) Colocalization of antigen or adjuvant with the stained macrophages was analyzed by Pearson's correlation. (*F*) Clodronate liposomes were injected into C57BL/6J mice either 2 or 7 d before immunization (*n* = 4). Mice were administered OVA (100 μg) plus K3-SPG (10 μg) at day 0. Eight days after immunization, OVA-specific serum IgG and IFN-γ were monitored. (*G*) C57BL/6J and *Tlr9*$^{-/-}$ mice were administered s.c. with K3 (10 μg) or K3-SPG (10 μg). At 24 h postadministration, the LNs were collected and the prepared cells were stained and analyzed by flow cytometry. (Scale bars, 100 μm.) *P < 0.05 (*t* test or Mann–Whitney *U* test). Data represent one of two or three independent experiments with similar results.

- 25 -

MARCO$^+$ macrophages in the LNs after injection, the macrophages were dispensable to inducing adaptive immune responses. In other words, the adjuvant effect of K3-SPG was largely dependent on the DC population.

K3-SPG Targets and Strongly Activates the Antigen-Bearing DC Population in Vivo.

Our findings suggest that although a large portion of nanoparticulate K3-SPG was taken up by MARCO$^+$ macrophages in iLNs after injection, the adjuvant effects appear to be controlled by DCs. We focused on antigen and adjuvant uptake by the DC population in iLNs. At 24 h postinjection, the uptake of antigen and adjuvants by the DC population was analyzed by flow cytometry. The frequency of CpG-positives in three DC subsets (pDCs, CD8α$^+$ DCs, and CD8α$^-$ DCs) was significantly increased after K3-SPG injection than with K3 (Fig. S8A). In contrast, the frequency of OVA-positive DCs was comparable after K3 and K3-SPG injections (Fig. S8B). When we focused on both antigen- and adjuvant-positive DCs, there was a substantial increase for K3-SPG over K3 (Fig. S9). Both pDCs and CD8α$^+$ DCs in iLNs were strongly activated by K3-SPG but not by K3 24 h postinjection, and this was completely dependent on TLR9 (Fig. 5G). Our results indicate that pDCs and CD8α$^+$ DCs preferentially capture nanoparticulate K3-SPG rather than nonparticulate K3 for maturation and to exert adjuvant effects.

K3-SPG Is a Potent Adjuvant for Influenza Vaccine in Murine and Nonhuman Primate Models.

Finally, we sought the adjuvant effect of K3-SPG by using more clinically relevant influenza vaccination models in both mice and nonhuman primates. When mice were immunized with ether-treated hemagglutinin antigen-enriched virion-free split vaccine (SV) plus the indicated adjuvant, K3-SPG demonstrated superior adjuvant effects to K3 when antibody responses (Fig. S10A) and T-cell responses (Fig. S10B) were compared. More importantly, SV plus K3-SPG immunization resulted in a 100-fold greater antibody response, even compared with vaccination using a whole (virion) inactivated vaccine (WIV) (0.2 μg per mouse) (Fig. 6A), which contains viral RNA as a built-in adjuvant (21). Interestingly, SV (0.1 μg per mouse) plus K3-SPG strongly induced both CD8 and CD4 T-cell responses (Fig. 6B). Mice immunized with SV and K3-SPG exhibited less body weight loss than WIV-immunized mice (Fig. 6C). Strikingly, K3-SPG conferred 100% protection against lethal PR8 virus challenge at the dose of which only 10% of WIV-vaccinated mice survived (Fig. 6D). These results strongly support the notion that K3-SPG works as a potent adjuvant for protein or protein-based vaccines in a murine model, prompting us to extend this finding to a nonhuman primate model using the cynomolgus monkey (*Macaca fascicularis*). Each group of three cynomolgus monkeys was immunized with SV plus K3 or K3-SPG at days 0 and 14. Serum antibody titers were then monitored for 8 wk. The SV plus K3-SPG induced significantly higher antibody titer at 2 wk postimmunization, and titer levels remained high for at least another 6 wk (Fig. 6E). Although antibody titers were reduced at 110 wk after immunization, the K3-SPG group had higher antibody titers than the K3 group (Fig. 6E). When PBMCs were stimulated with SV and WIV, IFN-γ was detected from the SV plus K3-SPG–immunized group (Fig. 6F). Taken together, these results suggest that K3-SPG is a prominent vaccine adjuvant in a nonhuman primate model.

Discussion

The medical need for novel, potent, and safe adjuvants is ever-increasing these days as (*i*) recombinant vaccine antigens such proteins and peptides are short on natural adjuvants, unlike attenuated or inactivated whole microbial antigens, (*ii*) conventional aluminum salts and oil adjuvants are limited or preferred for enhancing humoral immune responses, and (*iii*) new adjuvants that can induce cellular immune responses, including CTLs, are needed, for example for cancer vaccines. The last two decades have resulted in tremendous progress with respect to adjuvant research and development. A hallmark of the new gen-
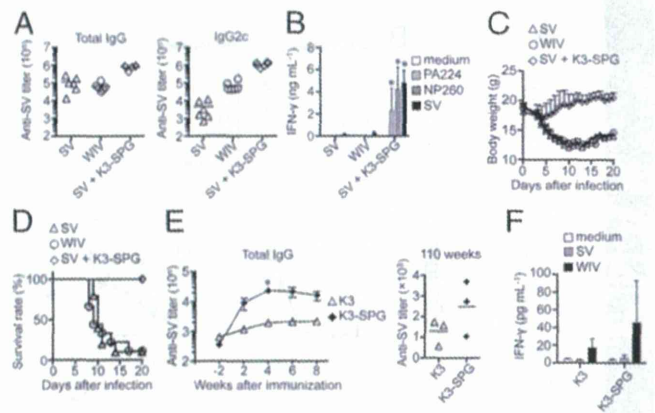

Fig. 6. K3-SPG acts as an influenza vaccine adjuvant in mice and nonhuman primates. (*A–D*) C57BL/6J mice (*n* = 6 or 10) were immunized with SV (0.1 μg), whole inactivated vaccine (WIV) (0.2 μg), or SV (0.1 μg) plus K3-SPG (10 μg) at days 0 and 14. Seven days after the final immunization, SV-specific serum IgG titers (*A*) and IFN-γ (*B*) [specific to SV antigen, PA$_{224-233}$ (PA224) (10 μg/mL) or NP$_{260-283}$ (NP260)] were monitored. (*C* and *D*) Fourteen days after the final immunization, mice were challenged with a 10-LD$_{50}$ dose of influenza virus A/PR/8 (H1N1). Changes in body weights (*C*) and mortality (*D*) were monitored for the next 20 d. (*E* and *F*) Cynomolgus monkeys (*n* = 3) were immunized with SV (5 μg) plus K3 (5 nmol) or SV plus K3-SPG (5 nmol) at days 0 and 14. (*E*) Serum samples were collected at −2, 2, 4, 6, 8, and 110 wk. Antigen-specific serum antibody titers were measured by ELISA. (*F*) PBMCs were prepared from individual cynomolgus monkey blood at 4 wk after the first immunization and restimulated in vitro with medium, SV (10 μg), or WIV for 24 h. Mouse IFN-γ in the supernatants was determined by ELISA. *P < 0.05 (*t* test or Mann–Whitney *U* test).

eration of adjuvants is that nucleic acids have been rediscovered to be immunologically active in stimulating specific innate immune receptors of the host, in particular TLRs. CpG DNA, a ligand for TLR9, is one of the most promising immunotherapeutic agents that has been identified.

Although there are several types of potent humanized CpG ODN—K (also called B), D (A), C, and P types—the development of an all-in-one CpG ODN activating both B cells and pDCs to form a stable nanoparticle without aggregation has been less than successful. In this study, we generated a novel K CpG ODN that we designated K3-SPG. Although it had been reported that there are molecular interactions between single-stranded nucleic acids and β-glucan (37) and that murine and humanized CpG ODNs can be wrapped by SPG to increase their original TLR9-agonistic activities (20), our report demonstrates that a rod-shaped nano-sized K3-SPG particle exhibits dual characteristics of K and D CpG ODNs (Fig. 1). K3-SPG is distinct from other previously reported K CpG ODNs, including K3. In turn, K3-SPG becomes a D CpG ODN, stimulating human PBMCs to produce large amounts of both type I and type II IFN, targeting the same endosome where the IFN-inducing D type resides without losing its K-type activity (Fig. 1 *F* and *G*). Another surprising finding is that this K3-SPG forms a rod-like single nanomolecule (Fig. 1 *C* and *D*). This is advantageous over previously demonstrated D or P types, whose ends form higher-order structures that may hamper further development as prodrugs, including good manufacturing practice assignment.

Another prominent feature of this K3-SPG is its potency as an adjuvant for induction of both humoral and cellular immune responses, especially CTL induction, to coadministered protein antigens without conjugation. Such potent adjuvant activity of K3-SPG is attributable to its nanoparticulate nature (Figs. 1 *C* and *D* and 2) rather than targeting Dectin-1 by SPG (Figs. 3 and 4). Initially, we hypothesized that K3-SPG becomes such a potent adjuvant because it targets Dectin-1, because SPG is a β-1,3-glucan, and seems to be a clear Dectin-1 ligand (Fig. 3A). Our other results, however, led us to conclude that the role of Dectin-1

- 26 -

in vivo with respect to the adjuvant activity of K3-SPG was minimal (Fig. 4). More importantly, the in vivo activity of K3-SPG was completely dependent upon TLR9 (Fig. 4 *E–G*). SPG is a soluble Dectin-1 ligand but not a Dectin-1 agonist, and thus does not interfere with TLR9-mediated DC activation (Fig. 3 *D* and *E*). The adjuvant activity of K3-SPG is mostly independent of Dectin-1, except at very low doses during the immunization protocol (Fig. 4*I*). Instead, some other receptors such as C-type lectins, Siglecs, and scavenger receptors may play roles in delivering SPG into macrophages and/or DCs, accumulating and activating antigen-bearing macrophages and DCs in draining lymph nodes (Fig. 5). In this regard, we also found that MARCO$^+$, but not Siglec-1$^+$, macrophages in draining lymph nodes are dominant in capturing K3-SPG, and coadministered antigen (LPS-free OVA protein), and that K3-SPG targets the antigen-bearing DC population in vivo. Although the depletion of macrophages did not ameliorate adjuvant effects, large amounts of antigen and K3-SPG are taken up by the same MARCO$^+$ macrophages, and the two-photon microscopic data suggest that they are activated as they become much bigger than nonstimulated macrophages. Whether this massive accumulation of antigen and adjuvant in MARCO$^+$ macrophages contributes to the following DC activation and adaptive T- and B-cell activation is yet to be elucidated in future work.

The protective potency of K3-SPG as an influenza vaccine adjuvant was demonstrated in vivo in both murine and non-human primate models. In the murine model, intradermal immunization with a very low dose of seasonal influenza split vaccine mixed with K3-SPG in solution provoked robust IgG responses and offered better protection than a low but physiological dose of whole inactivated virion vaccination against the heterologous challenge of lethal virus (Fig. 6 *C* and *D*). These data provide better protective potency than our previous results, where we used approximately 10 times higher doses of influenza antigens (21), because many factors for K3-SPG have been improved for its potency: K3–SPG complexation efficiency and optimization of the order between K3 and poly(dA$_{40}$) (Fig. 1); the immunization route is different as well. The data above prompted us to develop K3-SPG as a potent adjuvant for influenza split vaccine, especially for those urgently needing improvement: seasonal influenza vaccination for the elderly, immunodeficient patients (transplant recipients), and pandemic influenza vaccination.

Taken together, these data suggest that K3-SPG can be used as a potent adjuvant for protein vaccines such as influenza split vaccines, and may be useful for immunotherapeutic applications that require type I and type II IFN as well as CTL induction.

Materials and Methods

All animal studies using mice and monkeys were conducted in accordance with the Institutional Animal Care and Use Committee at the National Institute of Biomedical Innovation. All of the ODNs used in this manuscript were synthesized by GeneDesign. Other details are described in *SI Materials and Methods*.

1. Hemmi H, et al. (2000) A Toll-like receptor recognizes bacterial DNA. *Nature* 408(6813):740–745.
2. Krieg AM (2006) Therapeutic potential of Toll-like receptor 9 activation. *Nat Rev Drug Discov* 5(6):471–484.
3. Chu RS, Targoni OS, Krieg AM, Lehmann PV, Harding CV (1997) CpG oligodeoxynucleotides act as adjuvants that switch on T helper 1 (Th1) immunity. *J Exp Med* 186(10):1623–1631.
4. Brazolot Millan CL, Weeratna R, Krieg AM, Siegrist CA, Davis HL (1998) CpG DNA can induce strong Th1 humoral and cell-mediated immune responses against hepatitis B surface antigen in young mice. *Proc Natl Acad Sci USA* 95(26):15553–15558.
5. Klinman DM (2004) Immunotherapeutic uses of CpG oligodeoxynucleotides. *Nat Rev Immunol* 4(4):249–258.
6. Vollmer J, Krieg AM (2009) Immunotherapeutic applications of CpG oligodeoxynucleotide TLR9 agonists. *Adv Drug Deliv Rev* 61(3):195–204.
7. Krug A, et al. (2001) Identification of CpG oligonucleotide sequences with high induction of IFN-alpha/beta in plasmacytoid dendritic cells. *Eur J Immunol* 31(7):2154–2163.
8. Verthelyi D, Ishii KJ, Gursel M, Takeshita F, Klinman DM (2001) Human peripheral blood cells differentially recognize and respond to two distinct CpG motifs. *J Immunol* 166(4):2372–2377.
9. Hartmann G, Krieg AM (2000) Mechanism and function of a newly identified CpG DNA motif in human primary B cells. *J Immunol* 164(2):944–953.
10. Hartmann G, et al. (2003) Rational design of new CpG oligonucleotides that combine B cell activation with high IFN-alpha induction in plasmacytoid dendritic cells. *Eur J Immunol* 33(6):1633–1641.
11. Marshall JD, et al. (2003) Identification of a novel CpG DNA class and motif that optimally stimulate B cell and plasmacytoid dendritic cell functions. *J Leukoc Biol* 73(6):781–792.
12. Samulowitz U, et al. (2010) A novel class of immune-stimulatory CpG oligodeoxynucleotides unifies high potency in type I interferon induction with preferred structural properties. *Oligonucleotides* 20(2):93–101.
13. Kerkmann M, et al. (2005) Spontaneous formation of nucleic acid-based nanoparticles is responsible for high interferon-alpha induction by CpG-A in plasmacytoid dendritic cells. *J Biol Chem* 280(9):8086–8093.
14. Klein DC, Latz E, Espevik T, Stokke BT (2010) Higher order structure of short immunostimulatory oligonucleotides studied by atomic force microscopy. *Ultramicroscopy* 110(6):689–693.
15. Puig M, et al. (2006) Use of thermolytic protective groups to prevent G-tetrad formation in CpG ODN type D: Structural studies and immunomodulatory activity in primates. *Nucleic Acids Res* 34(22):6488–6495.
16. McHutchison JG, et al. (2007) Phase 1B, randomized, double-blind, dose-escalation trial of CPG 10101 in patients with chronic hepatitis C virus. *Hepatology* 46(5):1341–1349.
17. Bode C, Zhao G, Steinhagen F, Kinjo T, Klinman DM (2011) CpG DNA as a vaccine adjuvant. *Expert Rev Vaccines* 10(4):499–511.
18. Okamura K, et al. (1986) Clinical evaluation of schizophyllan combined with irradiation in patients with cervical cancer. A randomized controlled study. *Cancer* 58(4):865–872.
19. Sakurai K, Mizu M, Shinkai S (2001) Polysaccharide—polynucleotide complexes. 2. Complementary polynucleotide mimic behavior of the natural polysaccharide schizophyllan in the macromolecular complex with single-stranded RNA and DNA. *Biomacromolecules* 2(3):641–650.
20. Shimada N, et al. (2007) A polysaccharide carrier to effectively deliver native phosphodiester CpG DNA to antigen-presenting cells. *Bioconjug Chem* 18(4):1280–1286.
21. Koyama S, et al. (2010) Plasmacytoid dendritic cells delineate immunogenicity of influenza vaccine subtypes. *Sci Transl Med* 2(25):25ra24.
22. Minari J, et al. (2011) Enhanced cytokine secretion from primary macrophages due to Dectin-1 mediated uptake of CpG DNA/β-1,3-glucan complex. *Bioconjug Chem* 22(1):9–15.
23. Bae AH, et al. (2004) Rod-like architecture and helicity of the poly(C)/schizophyllan complex observed by AFM and SEM. *Carbohydr Res* 339(2):251–258.
24. Costa LT, et al. (2004) Structural studies of oligonucleotides containing G-quadruplex motifs using AFM. *Biochem Biophys Res Commun* 313(4):1065–1072.
25. Gürsel M, Verthelyi D, Gürsel I, Ishii KJ, Klinman DM (2002) Differential and competitive activation of human immune cells by distinct classes of CpG oligodeoxynucleotide. *J Leukoc Biol* 71(5):813–820.
26. Guiducci C, et al. (2006) Properties regulating the nature of the plasmacytoid dendritic cell response to Toll-like receptor 9 activation. *J Exp Med* 203(8):1999–2008.
27. Herre J, et al. (2004) Dectin-1 uses novel mechanisms for yeast phagocytosis in macrophages. *Blood* 104(13):4038–4045.
28. Goodridge HS, et al. (2011) Activation of the innate immune receptor Dectin-1 upon formation of a 'phagocytic synapse.' *Nature* 472(7344):471–475.
29. Eberle ME, Dalpke AH (2012) Dectin-1 stimulation induces suppressor of cytokine signaling 1, thereby modulating TLR signaling and T cell responses. *J Immunol* 188(11):5644–5654.
30. Saijo S, et al. (2007) Dectin-1 is required for host defense against *Pneumocystis carinii* but not against *Candida albicans. Nat Immunol* 8(1):39–46.
31. Martinez-Pomares L, Gordon S (2012) CD169$^+$ macrophages at the crossroads of antigen presentation. *Trends Immunol* 33(2):66–70.
32. Aoshi T, et al. (2009) The cellular niche of *Listeria monocytogenes* infection changes rapidly in the spleen. *Eur J Immunol* 39(2):417–425.
33. Gray EE, Cyster JG (2012) Lymph node macrophages. *J Innate Immun* 4(5-6):424–436.
34. Suzuki K, Grigorova I, Phan TG, Kelly LM, Cyster JG (2009) Visualizing B cell capture of cognate antigen from follicular dendritic cells. *J Exp Med* 206(7):1485–1493.
35. Gonzalez SF, et al. (2010) Capture of influenza by medullary dendritic cells via SIGN-R1 is essential for humoral immunity in draining lymph nodes. *Nat Immunol* 11(5):427–434.
36. Aoshi T, et al. (2008) Bacterial entry to the splenic white pulp initiates antigen presentation to CD8$^+$ T cells. *Immunity* 29(3):476–486.
37. Sakurai K, Shinkai S (2000) Phase separation in the mixture of schizophyllan and poly (ethylene oxide) in aqueous solution driven by a specific interaction between the glucose side chain and poly(ethylene oxide). *Carbohydr Res* 324(2):136–140.

IMMUNOLOGY